Journal of the Iranian Chemical Society
https://doi.org/10.1007/s13738-019-01766-4

ORIGINAL PAPER

Synthesis, crystal structure, antimicrobial activity and docking studies of new imidazothiazole derivatives

M. Koudad[1,2] · C. El Hamouti[3] · A. Elaatiaoui[1,2] · S. Dadou[1,2] · A. Oussaid[1,2] · F. Abrigach[1] · G. Pilet[4] · N. Benchat[1] · M. Allali[5]

Received: 31 January 2019 / Accepted: 12 August 2019

Abstract
A series of imidazothiazole derivatives were synthesized via Claisen–Schmidt condensation of aldehyde **3**, and different methyl ketones and their chemical structures were confirmed using ^{13}C NMR, ^{1}H NMR and LC–MS. In addition, the molecular structure of compound **3** was defined by single-crystal X-ray diffraction. The antibacterial and antifungal activities of synthesized compounds were investigated by diffusion method against three pathogenic bacteria (*Pseudomonas aeruginosa, Escherichia coli* and *Staphylococcus aureus*) and one pathogenic fungus (*Fusarium oxysporum*). Compound **3** displayed significant antibacterial activity against *E. coli* and *P. aeruginosa* (MIC ≤ 0.2 mg/ml). Concerning the antifungal activity, all the molecules show very interesting results versus *F. oxysporum* (IC_{50} ≤ 0.07 mg/ml). These results were confirmed by the molecular docking studies such as some compounds showing optimum binding energy and affinity to the active site of the receptor.

Keywords Imidazothiazole · Antibacterial · Antifungal · Molecular docking

Introduction

Recently, the fused heterobicyclic systems containing bridgehead nitrogen atom find an enormous importance in medicinal chemistry and health because of their interesting chemical, biological and pharmacological properties. Indeed, imidazothiazole derivatives are especially attractive because of the nitrogen-containing heterocyclic ring (present in natural products like histidine, biotin, nucleic acid, purine, etc.) and exhibit a wide spectrum of biological activity and pharmacological diversity, such as inhibition of some specific enzymes, anthelmintic [1], anti-inflammatory [2], antibacterial [2], fungistatic [3], antioxidant [4] and anticancer [5, 6]. Many studies report favorable biological properties of the imidazo[2,1-b]thiazole derivatives, especially anticancer activity against different kinds of human cancer cells [5, 6]. Among these active imidazo[2,1-b]thiazole derivatives are the immunomodulator and anthelmintic agent levamisole **1** and the anticancer agent YM-201627 **2a** (Scheme 1), an *N*,*N*-diethyl-2-(3-imidazo[2,1-b] [1, 3] benzothiazol-2-ylphenoxy)ethanamine dihydrochloride [6, 7]. The imidazo[2,1-b]thiazol-naphthamide **2b** (Scheme 1) has been described as a SIRT1-activating compound [8, 9]. In the last years, various derivatives of thiazole and imidazo[2,1-b] benzothiazole have been developed and described as having anticancer activity such as 3,6-diphenylimidazo[2,1-b] thiazole derivatives (**2c**) [10–12] (Scheme 1).

Finally, there is a considerable effort to develop a new efficient and inexpensive method to synthesize chalcones [13–17]; several synthetic methods are available in the literature. The most used is the Claisen–Schmidt

Electronic supplementary material The online version of this article (https://doi.org/10.1007/s13738-019-01766-4) contains supplementary material, which is available to authorized users.

✉ M. Allali
mallali.ispits.fes@gmail.com

1 LCAE, Faculty of Sciences, University Mohammed Premier, Oujda, Morocco

2 Department of Chemistry, Polydisciplinary Faculty of Nador, University Mohammed Premier, Oujda, Morocco

3 LPGE, Faculty of Sciences, University Mohammed Premier, Oujda, Morocco

4 Laboratoire des Multimatériaux et Interfaces (LMI), Université Claude Bernard Lyon 1, Villeurbanne, France

5 Institute of Nursing Professions and Health Techniques of Fez, 30000 Fez, Morocco

Published online: 24 August 2019

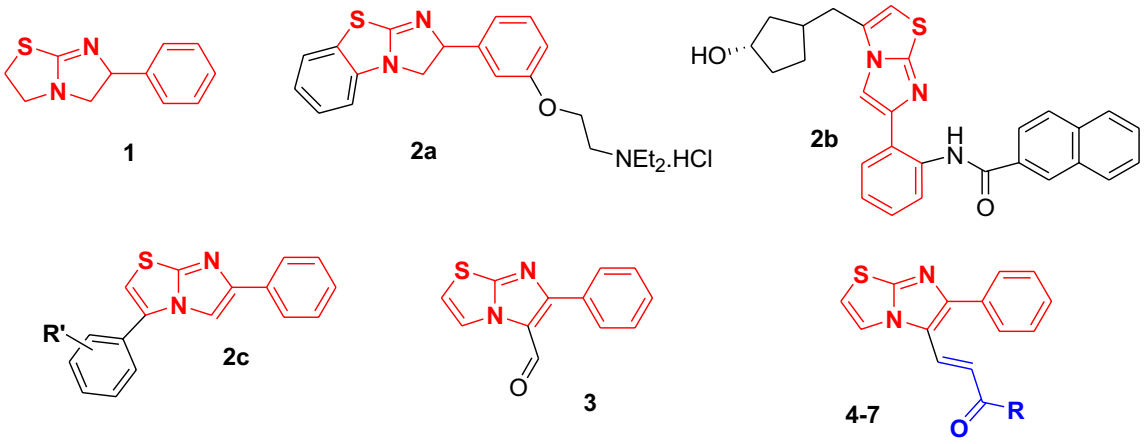

Scheme 1 Structures of some biologically active (**1**–**2**) and synthesized (**3**–**7**) imidazo[2,1-b]thiazole derivatives

condensation, which is the oldest, simplest and most frequently used reaction for chalcone synthesis. This process consists in condensing equimolar methyl aryl ketone amounts with an aryl aldehyde in an alcoholic medium and in the presence of a base [13].

As part of our program focusing on the discovery of novel biologically active compounds and in light of the above considerations, the extension of our previous work on the search for new biologically powerful molecules has been reported here [18]; in our search for novel biologically potent molecules, the synthesis and characterization of new compounds possessed an imidazo[2,1-b]thiazole scaffold and assessed their antimicrobial activities against three pathogenic bacteria (*Pseudomonas aeruginosa, Escherichia coli and Staphylococcus aureus*) and one pathogenic fungus (*Fusarium oxysporum*). Ciprofloxacin was used as positive control for antibacterial activity and Amoxicillin for antifungal activity, and DMSO was used as negative control.

To study the binding orientation to their protein targets, some compounds were docked in order to help in the prediction of the affinity/activity of the molecule.

Results and discussion

Spectroscopic characterization

The synthetic strategies adopted for constructing the target molecules are illustrated in Scheme 2.

The synthetic method for the preparation of chalcone analogues employing Claisen–Schmidt condensation of the imidazo[2,1-b]thiazole carbaldehyde **3** and different methyl ketones was used. This condensation is the most widely

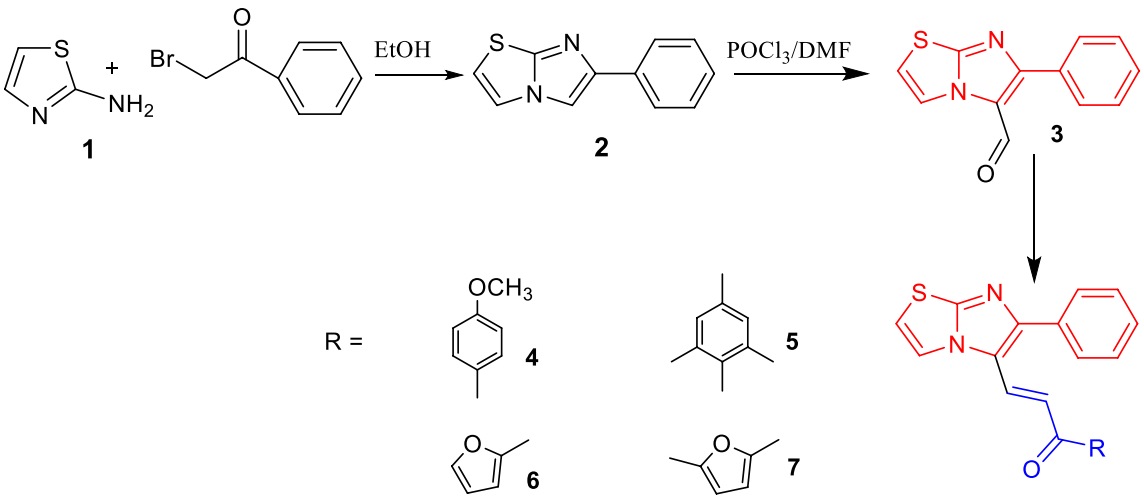

Scheme 2 Route synthesis of the ligands (**3**–**7**)

used method and is appreciated because of its relatively easy implementation, availability and acceptable yields of end products. This method has been previously reported [19]. The imidazo[2,1-b]thiazole carbaldehyde **3** was prepared by the following literature procedures [5]. The carbaldehyde **3** was generated using Vilsmeier–Haack [20] reaction from imidazo[2,1-b]thiazole **2**, DMF and $POCl_3$. Imidazo[2,1-b]thiazole **2** was obtained by cyclocondensation between 2-aminothiazole and an α-halogenated carbonyl compound, and this process was described by Hand and Paudler [21].

As shown in Scheme 2, a series of chalcone derivatives were prepared by the condensation of aromatic aldehyde **3** and different methyl ketones in methanol [22, 23]. As soon as the potassium hydroxide was added to the well-stirred mixture of aldehyde **3** and methyl ketones, desired unsaturated ketones (trans-alkene, E-form) were formed immediately as judged by ^{1}H NMR spectroscopy. Yields ranged between 74 and 82% without optimization.

To confirm the chemical structures of all the synthesized compounds, spectroscopic techniques were used. Indeed, ^{1}H NMR spectra of these compounds exhibit the expected characteristic protons. In the ^{1}H NMR spectra of compounds **4**, **5** and **7**, a singlet from 2.3 ppm to 4.3 ppm was found and was attributed to methyl protons (three methyl) and the multiplet between 6.7 and 8.4 ppm was ascribed to aromatic protons. Doublets corresponding to alkene protons were detected in the range of 6.80–8.20 ppm with aromatic protons. The resonance of different carbons at 110–160 ppm was attributed to aromatic carbons. The conjugated ketone's carbon was shielded and was assigned to the signal at 177 ppm in ^{13}C NMR spectra of **6** and **7**. The variation of the substituent of the same carbon induced the up-field shift in the frequencies to 186 ppm for **4** and 200 ppm for **5**.

The chemical structures of the synthesized imidazo[2,1-b]thiazole derivatives were confirmed by mass spectrometry. Further information about the isolation and full characterization of these compounds is provided in the "Experimental" section.

Compound **3** has been successfully crystallized, and its structure has been determined by single-crystal X-ray diffraction analysis. It crystallizes in the orthorhombic space group *P*bca.

A representative crystal structure is presented in Fig. 1. The crystal data and structural refinement of **3** are shown in Table 1. The imidazo[2,1-b]thiazole fragment is almost planar [RMS deviation = 0.003 Å], and the phenyl ring makes dihedral angle of [33.9(2)]° with this mean moiety. The crystal packing is stabilized by intermolecular C—H···N hydrogen bonds. As depicted in Table 2, most bond lengths were within the normal ranges: the C–C single bond is in the range of 1.339(2)–1.468(2) Å and the N–C bond lengths registered around 1.326(1) to 1.390(2) Å (see Table 1).

Figure 2 shows the stacking of the crystal structure of **3**. The layers develop in parallel planes along the *c*-axis, and the structure is stabilized by strong intermolecular bonds [C–H…N] and other van der Waals interactions forming a two-dimensional network of molecules connected to each other, thereby reinforcing the cohesion of the structure. Further information is available in supplementary data.

Antibacterial activity

The antibacterial activity related to action of the five components of the imidazothiazole derivatives **3**, **4**, **5**, **6** and **7** tested showed different inhibitory activities. According to the results shown in Table 2, the compound **3** showed a strong inhibitory effect against *Pseudomonas aeruginosa* and *E. coli* with a MIC ≤ 0.2 mg/ml and sensitivity against *S. aureus* (MIC ≤ 0.5 mg/ml). This may be due to the presence of a carbonyl oxygen atom which can form a hydrogen bond with the active site of the enzymes of the bacterium (Table 2).

Table 1 Hydrogen-bond geometry (Å, °)

D—H···*A*	*D*—H	H···*A*	*D*···*A*	*D*—H···*A*
C9—H91···N3	0.987	2.544	3.4416 (19)	151.13

Symmetry code: $x+1/2$, y and $-z+1/2$

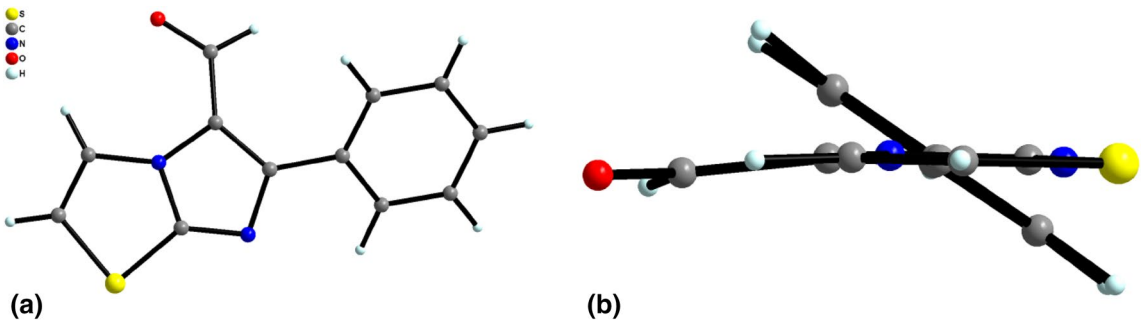

Fig. 1 **a** The molecular structure of **3**. **b** Dihedral angle of imidazothiazole ring with the phenyl ring in the crystal of **3**

Table 2 The diameter of inhibition and the MIC of five imidazothiazole compounds tested on three bacterial strains

Compound	Conc. of compound (µg/ml)	Bacterium					
		E. coli		*P. aeruginosa*		*S. aureus*	
		ID (mm)	MIC (µg/ml)	ID (mm)	MIC (µg/ml)	ID (mm)	MIC (µg/ml)
3	1000	15	200	16	200	12	500
	500	12		13		8	
	200	9		10		6	
	50	6		6		6	
6	1000	–	–	13	500	–	–
	500	–		10		–	
	200	–		6		–	
	50	–		6		–	
Ciprofloxacin				23	25		
Amoxicillin		22	20			22	19
Negative control		–	–	–	–	–	–
DMSO		–	–	–	–	–	–

ID inhibition diameter, *MIC* minimal inhibitory concentration, – no activity

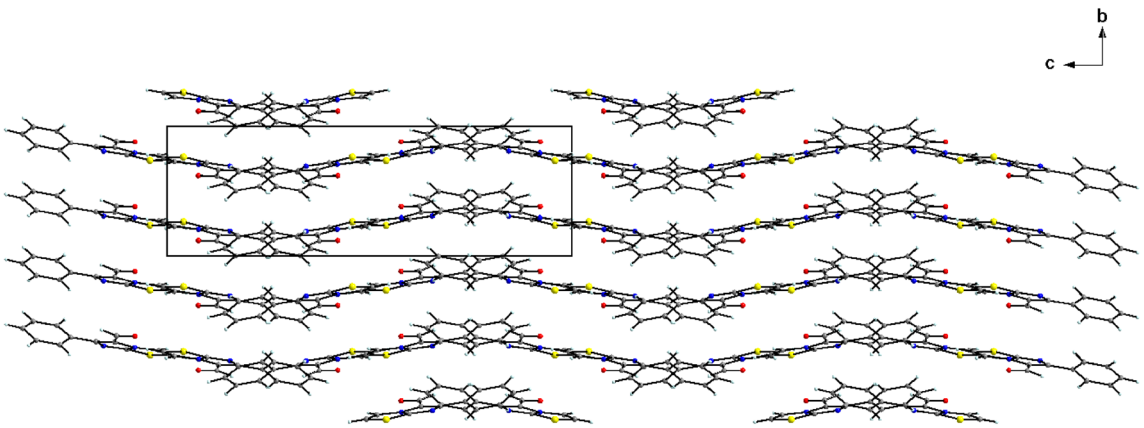

Fig. 2 The crystal packing of **3** viewed along the *b*–*c* axis

Compound **6** reveals activity against *P. aeruginosa* with an MIC ≤ 0.5 mg/ml. This activity may be due to the presence of furan oxygen, which can form a hydrogen bond with the amino acids. While the other ligands have no activity on the tested bacterial strains, this is probably due to the steric hindrance of these compounds which can prevent interactions with the active sites of the enzymes. To confirm these results, molecular docking was realized.

Antifungal activity

The antifungal test of the five imidazothiazole derivatives experienced at five different doses acted differently on the mycelia *F. oxysporum*. From Table 3, all the molecules showed very interesting results. Indeed, the mycelial growth is completely inhibited by **3**, **4**, **5**, **6** and **7** with IC_{50} not exceeding 0.07 mg/ml.

Molecular docking studies

The MOE program was used in this study because of the presence of various highly developed utilities and functions that allow us to give more realistic results, especially that concerning the calculation of protein–ligand binding free energy [score energy (S)]. This energy is calculated using a formalism taken into account the explicit hydrogens or electrostatic effects in computation [24, 25].

Thymidylate kinase (TMPK) is a crucial chemotherapeutic target due to its direct involvement in the synthesis of thymidine triphosphate, an essential component

Table 3 Growth inhibition rates (%) of the *Fusarium oxysporum* and IC_{50} values (mg/mL) for each product tested

Compound	Concentration (mg/mL)					IC_{50}(mg/ml)
	0.01	0.05	0.2	1	5	
3	20	50	81	97	100	0.05
4	15	47	78	93	100	0.07
5	30	65	95	100	100	0.02
6	16	47	80	97	100	0.06
7	20	48	80	95	100	0.05
Negative control	0	0	0	0	0	–
DMSO	0	0	0	0	0	–

Table 4 Docking results of the tested compounds

Compound	*S* (kcal/mol)	RMSD (Å)	Amino acids
0DF	−7.81	0.242	Gln105, Thr101 and Arg74
3	−6.59	0.887	Gln105 and Glu39
6	−4.02	0.949	Arg50 and Arg96

implicated in DNA replication, so inhibiting the function of this enzyme blocks DNA synthesis in replicating organisms [26, 27]. In fact, this enzyme catalyzes the conversion of thymidine 5′-monophosphate (dTMP) to thymidine 5′-diphosphate (dTDP) in the presence of ATP (adenosine triphosphate) and magnesium. Some known proposed inhibition mechanisms of TMPK enzymes are based essentially on the fact that the inhibitor affects the affinity of the enzyme for ATP by binding to the same site as ATP, not identical wholly or in part to the substrate-binding site for ATP, which makes the rate of formation of products slower, and thus results in the decrease in the catalytic activity of the enzyme. Actually, all the reported TMK inhibitors are thymidine analogues due to its cell permeability. Therefore, small-molecule TMK inhibitors, or nonsubstrate analogues, are necessary to develop antibacterial therapeutics. Herein, we report nonthymidine inhibitors targeting TMK enzyme in order to explain their antibacterial effect.

Based on the in vitro antibacterial screening, the two compounds **3** and **6** were docked into the active site of *Thymidylate kinase* protein to rationalize the experimental results and to evaluate its binding mode into the target enzyme. The docking score energy (S), RMSD values and interactions with amino acid residues of the studied compounds are summarized in Table 4.

The docking reliability was validated by re-docking co-crystallized ligand (0DF) into the binding site of *P. aeruginosa Thymidylate kinase*. A score of −7.81 kcal/mol was calculated for 0DF, and the predicted pose was similar to the experimental pose in the original crystal structure with a RMSD = 0.242 Å (Fig. 3). Predicted pose of the ligand 0DF showed H-bonding interactions with amino acid residues Gln105, Thr101 and Arg74 which are in total accordance with the experiment results.

The results of the molecular docking studies (Table 4) demonstrated that the two tested ligands interact with acid residues of *Thymidylate kinase* enzyme. Compound **3** showed a hydrogen bond formed between the oxygen of the carbonyl moiety and Gln105 with a distance equal to 1.86 Å. Also, it revealed a weak interaction between the sulfur atom and the amino acid Glu39 with a distance equal to 3.19 Å (Fig. 4). However, there are no interactions to the two residues Thr101 and Arg74. A strong docking score of about −6.59 kcal/mol was calculated, and it is comparable to the one obtained for the co-crystallized compound 0DF ($S = -7.81$ kcal/mol). From these results, we can postulate that **3** has a strong binding affinity to the active site of the receptor and also can exhibit a good and similar effect as 0DF.

The binding mode of compound **6** shows that the carbonyl group makes a hydrogen bond with Arg96 (distance = 2.04 Å), while the oxygen in the furan ring forms a hydrogen bond of 1.89 Å with the amino acid Arg50 (Fig. 5). Unfortunately, compound **6** formed no interactions similar to those displayed with 0DF. These observations may support the postulation that this compound may have a different effect to that observed by 0DF.

Experimental

Materials

The employed reagents were acquired from Aldrich and used without further purification. All the solvents were dried by adapted agents and distilled accordingly. The melting points were determined with a Tottoli apparatus. The ^{1}H and ^{13}C NMR were taken in $CDCl_3$ or $DMSOd_6$ using NMR Bruker Avance DPX 500 MHz spectrometer 500 MHz for ^{1}H and 126 MHz for ^{13}C. Chemical shifts δ are expressed in unit parts per million (ppm) and are still zeroed at tetramethyl silane (TMS) peak. Mass spectra have been performed on PerkinElmer SCIEX API 3000

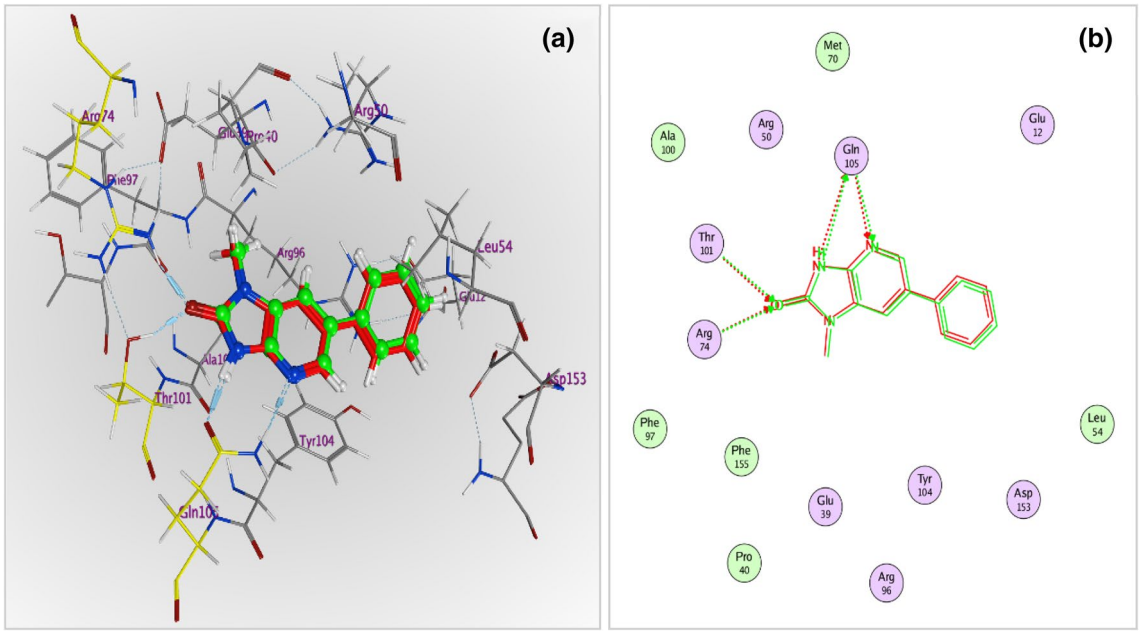

Fig. 3 3D (**a**) and 2D (**b**) superposition of predicted (green) and experimental (red) poses of the ligand 0DF into the binding site of *P. aeruginosa Thymidylate kinase*

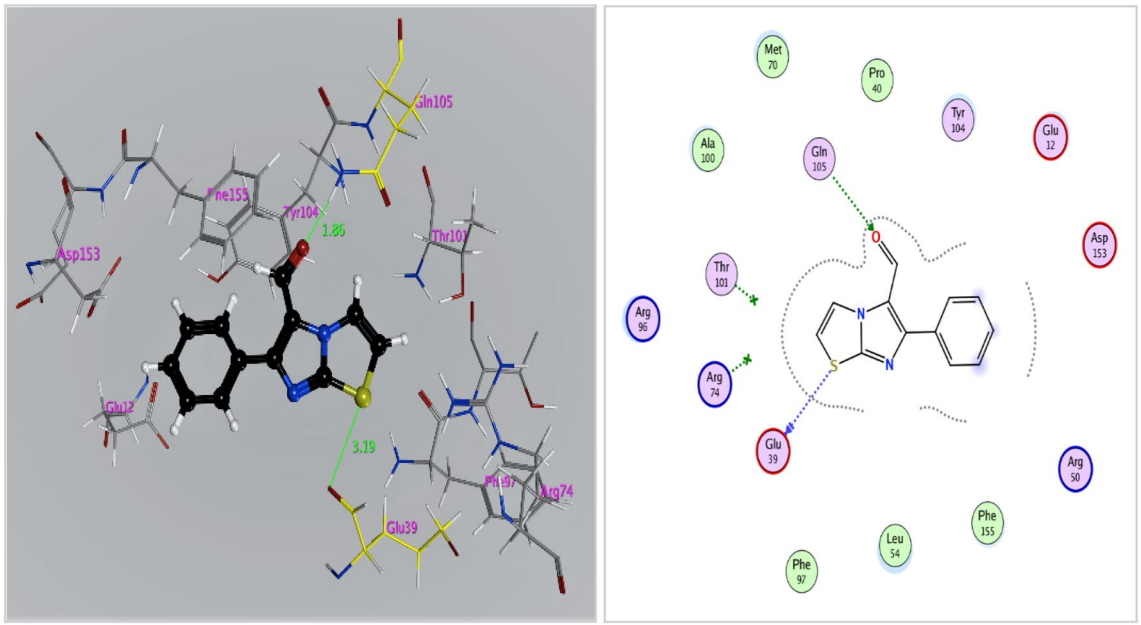

Fig. 4 3D and 2D interactions of **3** into the binding site of *P. aeruginosa* Thymidylate *kinase*

model. Thin layer chromatography (TLC) was used for monitoring reactions, using Merck silica gel 60 F254 precoated aluminum plates. UV light and I_2 were used for visualization. The chromatographic separations were carried out on silica gel columns (Merck, 60–120 mesh).

Synthesis

6-phenylimidazo[2,1-b]thiazole-5-carbaldehyde **3** This product is prepared by the following literature procedures [5].

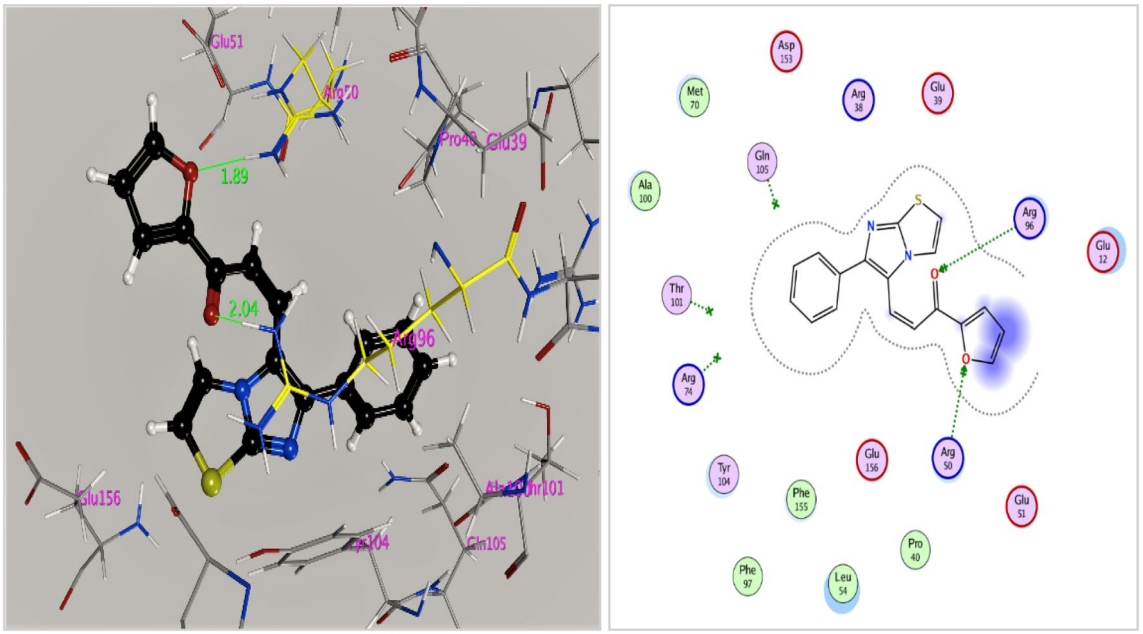

Fig. 5 3D and 2D interactions of compound **6** into the binding site of *P. aeruginosa* Thymidylate *kinase*

General procedure for the preparation of chalcone of imidazothiazole

To carbaldehyde **3** (0.5 mmol) in 15 ml of ethanol was added 1 ml of 10% aqueous KOH solution, and the mixture was stirred for 15–20 min at 60 °C. To this mass *p*-acetophenone (0.5 mmol) were added, and the mixture was stirred. The reaction was monitored by TLC. After 6–8 h, the mixture was poured in ice cold water and acetic acid was added for neutralization. Finally, the filtration gives the crude imidazothiazoles, which were purified by column chromatography on silica gel (ethyl acetate–hexane, 2:8) affording pure imidazothiazoles **4**–**7**.

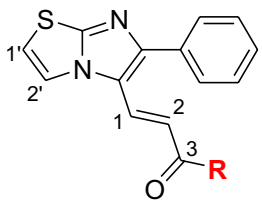

(E)-1-(4-methoxyphenyl)-3-(6-phenylimidazo[2,1-b] thiazol-5-yl)prop-2-en-1-one 4

Yellow solid from 4-methoxyacetophenone (74% Yield) Mp: 195–196 °C; ^{1}H NMR (500 MHz, DMSO-d_6) δ 8.72 (d, J = 4.6 Hz, 1H), 8.23–8.15 (m, 2H), 7.91 (d, J = 15.6 Hz, 1H), 7.76–7.66 (m, 2H), 7.59 (m, J = 27.2, 9.2, 6.2 Hz, 4H), 7.53–7.45 (m, 1H), 7.09 (d, J = 8.8 Hz, 2H), 3.85 (t, 3H, C$\underline{H}_3$); ^{13}C NMR (126 MHz, DMSO) δ 186.83, 163.09, 153.50, 152.52, 133.49, 130.91, 130.48, 128.79, 128.76, 128.66, 128.55, 121.71, 120.21, 116.01, 115.19, 113.88, 55.54; LC–MS: m/z = 361 (M + 1).

(E)-1-mesityl-3-(6-phenylimidazo[2,1-b]thiazol-5-yl) prop-2-en-1-one 5

Yellow solid from acetomesitylene (75% Yield); Mp: 200–201 °C; ^{1}H NMR (500 MHz, Chloroform-*d*) δ (ppm): 7.87 (d, J = 4.5 Hz, 1H), 7.62–7.52 (m, 3H), 7.47–7.35 (m, 3H), 6.92 (s, 2H), 6.71 (d, J = 16.4 Hz, 1H), 2.30 (d, J = 34.2 Hz, 10H); ^{13}C NMR (126 MHz, Chloroform-*d*) δ 200.58, 154.39, 153.78, 138.46, 136.91, 133.91, 133.23, 132.86, 128.76, 128.66, 128.43, 122.32, 119.65, 114.28, 21.15, 19.38; LC–MS: m/z = 373(M + 1).

(E)-1-(furan-2-yl)-3-(6-phenylimidazo[2,1-b]thiazol-5-yl) prop-2-en-1-one 6

Yellow solid from 2-acetylfuran (71% Yield); Mp: 170–171 °C; ^{1}H NMR (500 MHz, Chloroform-*d*) δ (ppm): 8.15 (d, J = 15.8 Hz, 1H), 7.94 (d, J = 4.5 Hz, 1H), 7.79–7.73 (m, 2H), 7.66 (dd, J = 1.7, 0.8 Hz, 1H), 7.57–7.49 (m, 2H), 7.50–7.43 (m, 1H), 7.34–7.29 (m, 1H), 7.26 (s, 1H), 7.10 (d, J = 4.5 Hz, 1H), 6.62 (dd, J = 3.6, J = 1.7 Hz, 1H); ^{13}C NMR (126 MHz, Chloroform-*d*) δ 177.64, 154.03, 153.95, 146.08, 133.52, 130.02, 129.10, 128.84, 120.61, 119.70, 116.87, 115.55, 114.13, 112.73; LC–MS: m/z = 321(M + 1).

(E)-1-(5-methylfuran-2-yl)-3-(6-phenylimidazo[2,1-b] thiazol-5-yl)prop-2-en-1-one 7

Yellow solid from 2-acetyl-5-methylfuran (82% Yield); Mp: 215–216 °C; ^{1}H NMR (500 MHz, Chloroform-*d*) δ (ppm): 8.45 (d, $J=7.5$ Hz, 1H), 7.88 (d, $J=15.2$ Hz, 1H), 7.71 (d, $J=7.5$ Hz, 1H), 7.60 (m, $J=5.7$, 2.4, 2.0 Hz, 2H), 7.42 (dp, $J=3.2$, 2.0 Hz, 3H), 7.24 (d, $J=7.3$ Hz, 1H), 6.69 (d, $J=15.0$ Hz, 1H), 6.29 (d, $J=7.5$ Hz, 1H), 2.39 (s, 3H); ^{13}C NMR (126 MHz, Chloroform-d) δ 177.03, 157.64, 153.61, 153.48, 152.73, 133.65, 129.50, 129.09, 128.82, 128.76, 120.63, 119.55, 118.89, 116.23, 113.99, 109.47, 14.27.; LC–MS: $m/z=335$ ($M+1$).

Antibacterial test

The antibacterial activity of five imidazothiazole derivatives **3**, **4**, **5**, **6** and **7** was evaluated by the diffusion method in agar medium on strains of *P. aeruginosa*, *E. coli* and *S. aureus* using the concentrations C_1: 1000 µg/ml; C_2: 500 µg/ml; C_3: 200 µg/ml and C_4: 50 µg/ml. The used test was that recommended by the NCCLS (National Committee for Clinical Laboratory Standards) and described by the AFNOR 2004: NF-U47-107.

From young colonies of 18–24 h, a bacterial suspension is carried out in sterile physiological water for each strain. The turbidity of this suspension is adjusted to 0.5 McFarland. This inoculum is seeded by flooding on Petri dishes containing Mueller–Hinton agar.

The Whatman paper disks (6 mm) are placed and soaked in the different tested compounds and then gently deposited on the surface of the agar. The same is true for ciprofloxacin disks against *P. aeruginosa*, Amoxicillin against *E. coli* and *S. aureus*. The Petri dishes are first left for 1 h at room temperature for prediffusion of the substances, before being incubated at 37 °C in an oven for 24 h. Antibacterial activity is determined by measuring the diameter of the inhibition zone around each disk to determine the lowest concentration of tested antimicrobial that inhibits the growth of the bacterium-tested MIC [28].

Antifungal test

The antifungal action of five imidazothiazole derivatives **3**, **4**, **5**, **6** and **7** is carried out on a *F. oxysporum* using the concentrations: C_1: 5 mg/ml; C_2: 1 mg/ml; C_3: 0.2 mg/ml; C_4: 0.05 mg/ml and C_5: 0.01 mg/ml.

Each compound was added to the potato dextrose agar (PDA) at different concentrations before culturing the fungus. Fungal cultures were incubated at 28 °C for 5 days. The inhibition percentage of each compound was calculated by the ratio of the mycelium diameter observed when using it over that observed in the negative control. IC_{50} was determined by the linear regression equation between the natural logarithm of the concentrations and the growth inhibition percentages [28].

X-ray data collection and structure determination

X-ray diffraction pattern of **3** was collected by using Oxford Diffraction Gemini diffractometer [29]. The experiments were performed at 293 K with Mo Kα radiation ($\lambda=0.71069$ Å). Cell refinement was carried out using *Chrysalis* [30]; program(s) used to solve structure: *SIR97* [31]; program(s) used to refine structure: CRYSTALS [32]; molecular graphics: CAMERON [33]; and software used to prepare material for publication: CRYSTALS [32]. Refinement of F^2 against all reflections. The weighted *R*-factor *wR* and goodness of fit *S* are based on F^2, and conventional *R*-factors *R* are based on *F*, with *F* set to zero for negative F^2. The threshold expression of $F^2>\sigma(F^2)$ is used only for calculating *R*-factors(gt), etc., and is not relevant to the choice of reflections for refinement. *R*-factors based on F^2 are statistically about twice as large as those based on *F*, and *R*-factors based on all data will be even larger.

Table 5 summarizes the pertinent crystallographic data and refinement details of **3**.

Table 5 Crystal data and structural refinement of compound **3**

Chemical formula	$C_{12}H_8N_2OS$
M_r	228.27
Temperature (K)	$T=293$ K
Crystal system, space group	Orthorhombic, *P b c a*
a, *b*, *c* (Å)	12.6730(4), 7.2844(3), 22.7774(9)
B (°), λ (Å)	97.449(12), 0.71069
V (Å^3)	2102.70(14)
Z	8
D_x (g/cm^3)	1.442
μ	0.284
F(000)	944
Crystal size (mm^3)	0.243×0.400×0.505
Radiation	Mo *K*α ($\lambda=0.71069$ Å)
θ range (°)	3.215–29.418
T_{min}/T_{max}	0.900/0.930
R_{int}	0.023
wR (F^2)	0.0439
$R[F^2>2\sigma(F^2)]$	0.0365
S (F^2)	1.063
Measured reflections/independent reflections/reflections with $I>2\sigma(I)$	12028/2589/2200
$\Delta\rho_{max}/\Delta\rho_{min}$ (Å^{-3})	0.19/−0.24

Molecular docking simulation

The ligand–protein docking study was performed using MOE (2014.09 software) [34]. The crystal structure of the *Thymidylate kinase* from *P. aeruginosa* bound with 1-methyl-6-phenyl-1,3-dihydro-2H-imidazo[4,5-b]pyridin-2-one (0DF) (PDB code: 3UWK) was retrieved from Protein Data Bank (http://www.rcsb.org/). Hydrogens were added, partial charges were calculated, and water molecules and cofactors were removed. Docking study was carried out following the standard protocol implemented in MOE (2014.09). Structure of the selected compounds was built in ACD/ChemSketch [35], and geometry was optimized with the semi-empirical Hartree–Fock AM1 method [36] using Gaussian software [37].

Conclusion

Five imidazothiazole derivatives were successfully synthesized with good yields by simple condensation between 2-aminothiazole and a differently substituted α-halogenated carbonyl compound. All new compounds were characterized by MS, ^{1}H and ^{13}C NMR. The in vitro antimicrobial activities of these imidazothiazole derivatives were evaluated against three bacterial strains (*P. aeruginosa, E. coli* and *S. aureus)* and one fungal strain (*F. oxysporum*). The preliminary results of these compounds against the studied microorganisms showed moderate-to-good antibacterial and antifungal activities. Indeed, **3** and **6** exhibited promising antimicrobial activity. Regarding the antifungal activity, all the molecules showed very interesting results versus *F. oxysporum.* These results were confirmed by a theoretical molecular docking study where it revealed that the two compounds **3** and **6** can make hydrogen bonds with many amino acid residues of the active site of *P. aeruginosa Thymidylate kinase* enzyme. The results of this study can support the postulation that the compound **3** can be a good candidate for the development of a new antibacterial inhibitor targeting *Thymidylate kinase* enzyme.

References

1. N.S. Shetty, I.A.M. Khazi, C. Ahn, Bull. Korean Chem. Soc. **31**, 2337 (2010)
2. A. Andreani, M. Granaiola, A. Leoni, A. Locatelli, R. Morigi, M. Rambaldi, V. Garaliene, W. Welsh, S. Arora, G. Farruggia, J. Med. Chem. **48**, 5604 (2005)
3. J. Robert, S. Boukraa, J. Panouse, V. Loppinet, J. Chaumont, Eur. J. Med. Chem. **25**, 731 (1990)
4. G.D. Kapche, C.D. Fozing, J.H. Donfack, G.W. Fotso, D. Amadou, A.N. Tchana, M. Bezabih, P.F. Moundipa, B.T. Ngadjui, B.M. Abegaz, Phytochemistry **70**, 216 (2009)
5. A. Kamal, D. Dastagiri, M.J. Ramaiah, J.S. Reddy, E.V. Bharathi, C. Srinivas, S. Pushpavalli, D. Pal, M. Pal-Bhadra, ChemMedChem **5**, 1937 (2010)
6. O. Dahl, Ø. Fluge, E. Carlsen, J.N. Wiig, H.E. Myrvold, B. Vonen, N. Podhorny, O. Bjerkeset, T.J. Eide, T.B. Halvorsen, Acta Oncol. **48**, 368 (2009)
7. A. Andreani, D. Bonazzi, M. Rambaldi, Arch. Pharm. **315**, 451 (1982)
8. E.-J. Kim, J.-H. Kho, M.-R. Kang, S.-J. Um, Mol. Cell **28**, 277 (2007)
9. C.B. Vu, J.E. Bemis, J.S. Disch, P.Y. Ng, J.J. Nunes, J.C. Milne, D.P. Carney, A.V. Lynch, J.J. Smith, S. Lavu, J. Med. Chem. **52**, 1275 (2009)
10. R.M. Kumbhare, K.V. Kumar, M.J. Ramaiah, T. Dadmal, S. Pushpavalli, D. Mukhopadhyay, B. Divya, T.A. Devi, U. Kosurkar, M. Pal-Bhadra, Eur. J. Med. Chem. **46**, 4258 (2011)
11. J.-H. Park, M.I. El-Gamal, Y.S. Lee, C.-H. Oh, Eur. J. Med. Chem. **46**, 5769 (2011)
12. S. Koppireddi, D.R.K. Chilaka, S. Avula, J.R. Komsani, S. Kotamraju, R. Yadla, Bioorganic Med. Chem. Lett. **24**, 5428 (2014)
13. F. Herencia, M.L. Ferrandiz, A. Ubeda, J. Domínguez, J.E. Charris, G.M. Lobo, M.J. Alcaraz, Bioorganic Med. Chem. Lett. **8**, 1169 (1998)
14. N.U. Güzeldemirci, Ö. Küçükbasmacı, Eur. J. Med. Chem. **45**, 63 (2010)
15. J.K. Malik, H. Soni, A. Singhai, J. Pharm. Res. **7**, 39 (2013)
16. E. Gürsoy, N.U. Güzeldemirci, Eur. J. Med. Chem. **42**, 320 (2007)
17. A. Andreani, M. Granaiola, A. Leoni, A. Locatelli, R. Morigi, M. Rambaldi, L. Varoli, D. Lannigan, J. Smith, D. Scudiero, Eur. J. Med. Chem. **46**, 4311 (2011)
18. M. Allali, G.T. Benjelloun, N. Chahboun, Y. Mouacha, N. Allali, L. Bennani, I. Ouahidi, J. Ibijbijen, L. Nassiri, J. Mater. Environ. Sci. **8**, 8 (2017)
19. R. Li, G.L. Kenyon, F.E. Cohen, X. Chen, B. Gong, J.N. Dominguez, E. Davidson, G. Kurzban, R.E. Miller, E.O. Nuzum, J. Med. Chem. **38**, 5031 (1995)
20. E. Öhler, E. Zbiral, M. El-Badawi, Tetrahedron Lett. **24**, 5599 (1983)
21. E.S. Hand, W. Paudler, Tetrahedron **38**, 49 (1982)
22. B. Shivarama Holla, S. Ambekar, J. Indian Chem. Soc. **50**, 673 (1973)
23. K. Kazauki, K. Htayama, S. Yokomor, T. Soki, Chem. Abstr. **85**, 5913 (1976)
24. J.B. Cross, D.C. Thompson, B.K. Rai, J.C. Baber, K.Y. Fan, Y. Hu, C. Humblet, J. Chem. Inf. Model. **49**, 1455 (2009)
25. C.R. Corbeil, C.I. Williams, P. Labute, J. Comput. Aided Mol. Des. **26**, 775 (2012)
26. J.Y. Choi, M.S. Plummer, J. Starr, C.R. Desbonnet, H. Soutter, J. Chang, J.R. Miller, K. Dillman, A.A. Miller, W.R. Roush, J. Med. Chem. **55**, 852 (2012)
27. S.C. Van, Verhandelingen-Koninklijke Academie voor Geneeskunde van Belgie **68**, 223 (2006)
28. T.R. Shryock, Performance standards for antimicrobial disk and dilution susceptibility tests for bacteria isolated from animals: approved standard, NCCLC2002
29. Oxford Diffraction, *CrysAlisPro* (Oxford Diffraction Ltd, Abingdon, England, 2006)
30. Oxford Diffraction, *CrysAlisPro* (Oxford Diffraction Ltd, Abingdon, Oxfordshire, England, 2010)
31. A. Altomare, M.C. Burla, M. Camalli, G.L. Cascarano, C. Giacovazzo, A. Guagliardi, A.G. Moliterni, G. Polidori, R. Spagna, J. Appl. Crystallogr. **32**, 115 (1999)

32. P.W. Betteridge, J.R. Carruthers, R.I. Cooper, K. Prout, D.J. Watkin, J. Appl. Crystallogr. **36**, 1487 (2003)
33. D. Watkin, C. Prout, J. Carruthers, P. Betteridge, *Crystals* (Chemical Crystallography Laboratory, Oxford U.K., 1996)
34. *Molecular Operating Environment Software* (Chemical Computing Group Inc, Montreal, Canada, 2014)
35. *ACD/ChemSketch* (Advanced Chemistry Development, Inc, Toronto, ON, Canada, 2011). http://www.acdlabs.com
36. M.J. Dewar, E.G. Zoebisch, E.F. Healy, J.J. Stewart, J. Am. Chem. Soc. **107**, 3902 (1985)
37. M.J. Frisch, G.W. Trucks, H.B. Schlegel, G.E. Scuseria, M.A. Robb, J.R. Cheeseman, G. Scalmani, V. Barone, B. Mennucci, G.A. Petersson, H. Nakatsuji, M. Caricato, X. Li, H.P. Hratchian, A.F. Izmaylov, J. Bloino, G. Zheng, J.L. Sonnenberg, M. Hada, M. Ehara, K. Toyota, R. Fukuda, J. Hasegawa, M. Ishida, T. Nakajima, Y. Honda, O. Kitao, H. Nakai, T. Vreven, J.A. Montgomery Jr., J.E. Peralta, F. Ogliaro, M.J. Bearpark, J. Heyd, E.N. Brothers, K.N. Kudin, V.N. Staroverov, R. Kobayashi, J. Normand, K. Raghavachari, A.P. Rendell, J.C. Burant, S.S. Iyengar, J. Tomasi, M. Cossi, N. Rega, N.J. Millam, M. Klene, J.E. Knox, J.B. Cross, V. Bakken, C. Adamo, J. Jaramillo, R. Gomperts, R.E. Stratmann, O. Yazyev, A.J. Austin, R. Cammi, C. Pomelli, J.W. Ochterski, R.L. Martin, K. Morokuma, V.G. Zakrzewski, G.A. Voth, P. Salvador, J.J. Dannenberg, S. Dapprich, A.D. Daniels, Ö. Farkas, J.B. Foresman, J.V. Ortiz, J. Cioslowski, D.J. Fox, *Gaussian 09* (Gaussian, Inc, Wallingford, 2009)